Application of a novel diffraction-based tomography method for imaging biological samples

Chaminda R. Samarage[a*], Gregory J. Sheard[b], Andreas Fouras[a]
[a]Laboratory for Dynamic Imaging, Department of Mechanical and Aerospace Engineering, Monash, University, Clayton, Melbourne, Australia
[b]Fluids Laboratory for Aeronautical and Industrial Research, Department of Mechanical and Aerospace Engineering, Monash, University, Clayton, Melbourne, Australia

ABSTRACT

A novel system to image and reconstruct a 3-dimensional map of the refractive index based on the diffraction of light through a transparent sample is presented. This method is tested and validated on computer-generated data sets. The proposed system is an advanced variation of an imaging technique used in engineering for the study of aerodynamics. This method, which is termed Reference Image Topography, is used to reconstruct the water/air interface of the free surface in fluid dynamics studies. This surface profile is reconstructed by comparing an image of a random pattern viewed through the transparent free surface against a reference image, to determine the change in the refractive index caused by changes in the height. The proposed system is highly sensitive and capable of imaging intricate features in the transparent sample that are of low contrast when imaged with other imaging methods. For each projection, the change in direction of the light passing through the sample when placed in between the light source and the imaging system, can be related to the line integral for the change in refractive index across the sample. Utilizing multiple projections, a 3-dimensional map of the refractive index of the sample is reconstructed with computed tomography.

Keywords: Computed tomography, refractive index, reference image, particle image velocimetry, RIT-CT

1. INTRODUCTION

The ability to capture quantitative 3-dimensional (3D) information of living biological samples is important for medical research[1]. With embryology, this is as important as current mutational and genomic approaches to understanding developmental processes. While there are confocal microscopic methods that can yield 3D images[2], for small embryo-sized samples, tomographic imaging methods are ideal as they offer non-intrusive measurements. While tomographic methods such as optical projection tomography[3] have been shown to yield favorable results in the visible light range of the spectrum, X-ray based tomography for developmental biology has been constrained by low X-ray absorption of tissue.

X-ray imaging is gaining interest amongst scientists as the primary means of imaging and investigating biological tissues[1], [4], [5]. Biological tissues have non-uniform refractive-index distributions and thicknesses that affect the wavefronts of passing X-rays. Phase contrast imaging[6] exploits these differences in the refractive indices between soft tissues. This provides images where different tissues are clearly distinguishable due to the differing phase changes caused by the tissue as the X-rays pass through a sample. However, most quantitative phase contrast imaging is done either by using interference of the object with a reference beam[7] or phase shifting interferometry[8]. Additionally, due to the low levels of exposure (dose) that is often required when imaging live biological samples, obtaining quantitative phase information with phase contrast imaging is difficult.

*rajeev.samarage@monash.edu.au; www.ldi.monash.edu.au

Developments in X-Ray Tomography VIII, edited by Stuart R. Stock,
Proc. of SPIE Vol. 8506, 85061I · © 2012 SPIE · CCC code: 0277-786/12/$18
doi: 10.1117/12.929444

Deflectometry is a method whereby phase information such as the thickness, position or the refractive index of a phase object could be determined by the way light interacts with the phase object, which is the fundamental concept behind methods such as Background Oriented Schlieren (BOS)[9], Reference Image Topography (RIT)[10], [11], and X-ray phase imaging[12], [13]. Massig[14] showed how the distortion of a periodic fringe pattern could be utilized to visualize a phase object. Perciante and Ferrari[15] extended this work for use with a two-dimensional (2D) reference pattern. The object is placed in between a 2D reference pattern and a digital camera and the ray deflections caused by the object are determined by comparing to an image of the reference pattern without the object in between. In aerodynamics, a similar concept was utilized to visualize the waves formed on the water surface as water passes a circular cylinder[10], [16], [17]. This method, termed Reference Image Topography[10], [11], [16–18] utilizes the distortion of a reference pattern caused by the water waves, to determine the change in refractive index and in turn reconstruct the surface profile of the water/air interface. Recently, a similar analogy was extended to X-rays[12], [19] where the thickness of polymethylacrylate spheres was reconstructed based on the distortion of a single attenuation grid[12] and the distortion of a random reference pattern[19]. Berujon et al[13] showed that a similar method could advance two-dimensional phase sensing techniques. They showed how quantitative phase information of an X-ray beam could be determined using an image of a speckle pattern caused by a biological filtering membrane and an image of the speckle pattern with a phase object in the beam path.

Atcheson et al[9] presented a Background Oriented Schlieren (BOS) based method to obtain volumetric, time-resolved refractive index measurements in a gas flame. The method uses 16 cameras to image a reference pattern that is being distorted by refractive index variations in the air. These variations are the result of temperature variations in the air brought about by the heat of the flame. Optical flow algorithms were used to quantitatively determine the distortion caused by the changes in the refractive index to the background reference. This distortion was shown to be proportional to the line integral of the refractive index gradient along the sample in the projection direction. A 3D map for the refractive index gradient was determined using computed tomography (CT). CT is a technique used to reconstruct an object in 3D space using 2D projections. With standard CT, the pixel intensities on the digital image are assumed to be proportional to the integrated object intensity in the projection direction. The structure of the object is reconstructed from projection images taken at different angles using back projection or algebraic reconstruction techniques[20]. Subsequently, Poisson integration is used to determine the refractive index map of the flame. Tomographic phase microscopy[21] utilizes an interferometric approach to obtain quanitative 3D maps for the refractive index inside living cells using visible light. While this method offers high spatial resolution (up to 0.5 microns in the transverse direction), the optical setup for tomographic phase microscopy is complex and cumbersome to setup.

We present a novel diffraction-based imaging method where quantitative 3D phase information can be readily obtained using a simple setup and allows for volumetric imaging of biological samples. The proposed method uses light efficiently as it does not use diffraction gratings[12], analyzer crystals[22] or complicated optical configurations[21]. This method combines an advanced variation of the Reference Image Topography method presented by Fouras et al[10] with CT and is capable of measurements over a wide range of wavelengths in the electromagnetic spectrum. The method presented here is mainly intended for imaging with X-rays or visible light.

2. A METHOD FOR REFRACTIVE INDEX MEASUREMENTS

The proposed system, which we term Reference Image Topography Computed Tomography (RIT-CT), works by imaging a random high-frequency interference pattern with a digital camera through a biological sample. The interference pattern is imaged with the digital camera and then imaged again after introducing the complex sample. The two images are analyzed using Particle Image Velocimetry (PIV) software to determine the degree by which the underlying pattern is distorted. With PIV, the two images are subdivided into regular regions called interrogation windows separated by a set sampling distance. This sampling distance could be altered for oversampled measurements. For each interrogation window, a digital cross-correlation is computed between the two sub-images in the interrogation region. The maximum of the resulting cross-correlation is representative of the underlying displacement. In this case, this displacement is the distortion caused by optical properties of the object in the light path. The high-frequency interference pattern is optimal for the cross-correlation analysis and hence optimal for an accurate measurement of the image distortion[23].

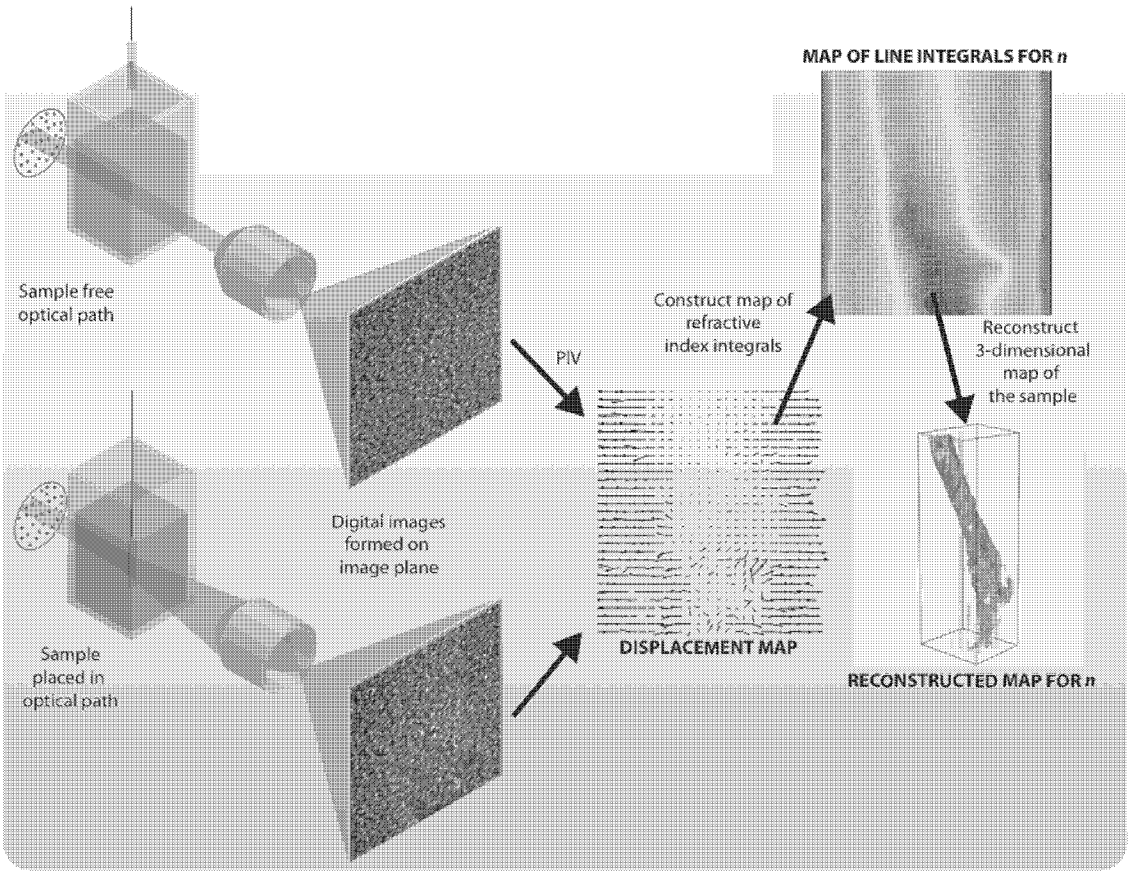

Figure 1. Graphical representation of the post-processing steps in the Reference Image Topography Computed Tomography (RIT-CT) method. A digital image is captured of the reference interference pattern without the biological sample in the optical path. The biological sample is then lowered into the bath of the immersion medium and rotated using the rotation stage. Digital images of the now distorted interference pattern are captured. For a single projection in the data sequence, Particle Image Velocimetry (PIV) is used to evaluate the distortion caused by the sample to the interference pattern. The displacement map is used in conjunction with an estimate for the sample depth, to estimate for a 2D map of the averaged refractive index over the respective sample depth. Utilizing these 2D maps of the refractive index for each projection in the dataset, a Simultaneous Algebraic Reconstruction Technique (SART) is used to reconstruct a 3D map of the refractive index.

Figure 1 shows a graphical flowchart of the processes involved to obtain quantitative refractive index measurements. This displacement field obtained from the cross-correlation analysis is analyzed using an advanced variation of the Reference Image Topography method introduced by Fouras et al[10], [11]. This modified version performs a ray trace to estimate the refractive index gradients in the projection image using the displacement measurements from cross-correlation analysis. A Fourier integration as discussed in Morgan et al[12] is used to integrate the refractive index gradients to obtain a map for the integral of the refractive index over the sample thickness. The sample is rotated using a rotation stage and multiple projections are captured. For each projection, the aforementioned processes are repeated to obtain multiple projections of refractive index integrals integrated over the sample thickness. Using CT, the map for the refractive index is recovered from the multiple projections.

Figure 2 shows the typical RIT-CT experimental setup for use with X-rays. The random pattern is illuminated with X-rays (red) and passes through the sample to interact with the scintillator to produce visible light (yellow). A microscope objective lens is used to magnify and focus the visible light onto the sensor in the digital camera. The sample would be mounted inside a glass capillary that is fixed to the rotation stage as shown in the inset A of figure 2. Biological samples are not typically transparent, with the exclusion of very young embryos where tissue pigmentation is yet to develop. While sample transparency does not affect imaging with X-rays, with visible light, the biological samples would need to be dehydrated and optically cleared using clearing agents such as Benzyl Alcohol Benzyl Benzoate or glycerol. In this case, the sample would be mounted inside a glass cylinder as shown in the inset (A) of figure 2 and immersed in the

clearing agent. As the method relies on optical distortion due to refractive index mismatch, care has to be taken in deciding the material of the glass capillary and clearing agent/immersion medium to reduce unwanted noise to the refractive index measurements.

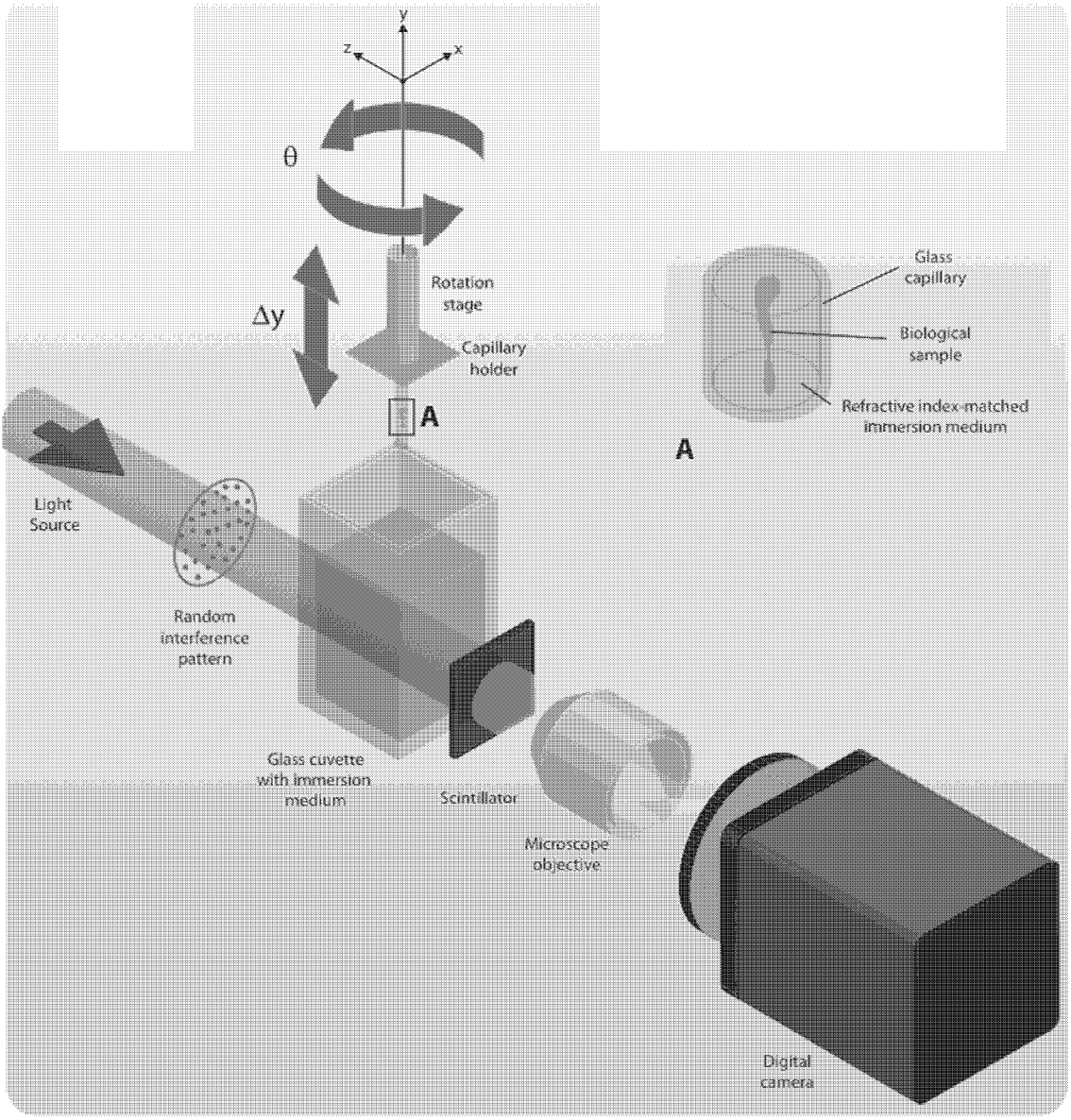

Figure 2. Graphical representation of the experimental configuration utilized in this implementation of the proposed diffraction-based tomography method, which we term Reference Image Topography Computed Tomography (RIT-CT). The light source (red) is used to back illuminate a random interference pattern, pass through the sample and interact with the scintillator to produce visible light (yellow). A microscope objective is used to magnify and focus the visible light to the digital camera. The digital camera is used to capture a single image of the illuminated random pattern and this is utilized as the reference image for the subsequent post-processing steps of RIT-CT (see figure 1). The sample, which is inside a glass capillary and attached to the rotation stage (as shown in the inset A), is lowered into the glass cuvette with the immersion medium. Images of the distorted reference pattern are captured for each projection in the acquisition while the rotation stage is rotated.

3. VALIDATION

The proposed RIT-CT method is validated using computer-generated images obtained from ray-tracing. First, the RIT-CT method is used to reconstruct the structure of a complex object that is completely transparent. The spatial resolution of the method is then evaluated using sine curve pairs and finally the method is applied to obtain 3D refractive index measurements of a phantom.

3.1 Image generation

Synthetic images are generated using Blender, a free open source 3D content creation suite with a host of ray-tracing engines. Ray-tracing is a technique by which realistic images can be created by tracing the path of light through a 3D scene that consists of 3D objects. Blender is set up similarly to the graphical representation shown in figure 2. A camera is focused on a plane that has a random computer generated speckle pattern and illuminated uniformly using white light. Using Blender's 3D meshing tools, the object can be meshed and optical parameters such as the refractive index can be modified. Using custom python scripts, the object is rotated and images are rendered at each projection angle. Unless specified, each projection image is 1024 × 1024 pixels in resolution and the model camera has a pixel size of 0.6 microns.

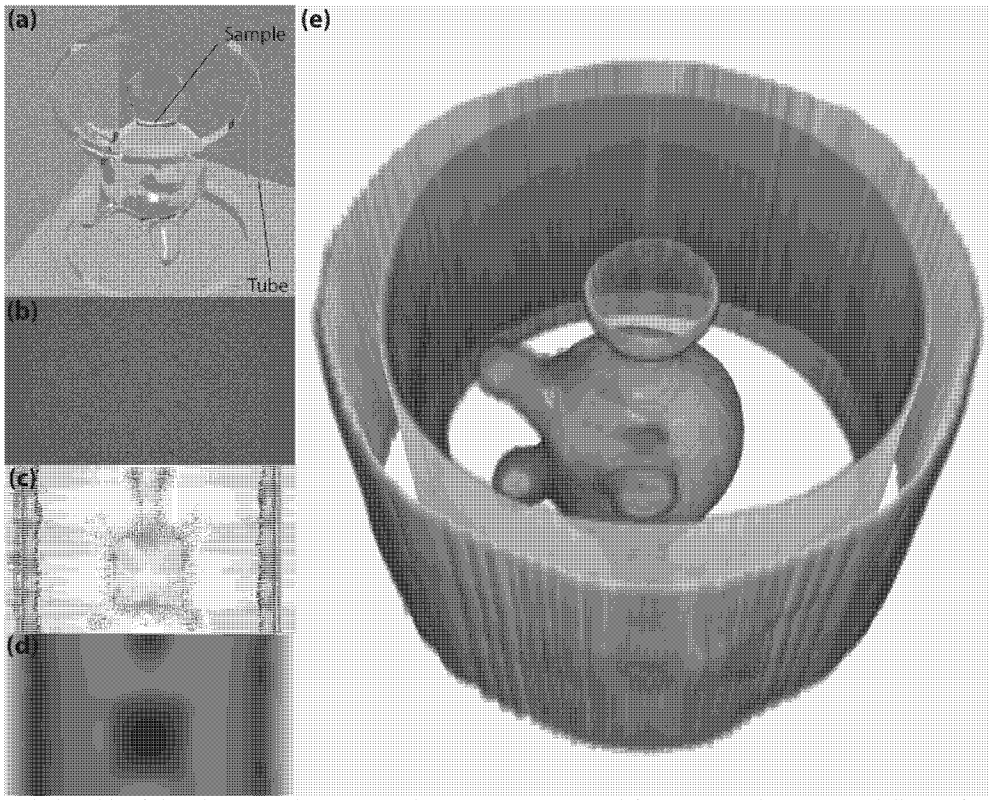

Figure 3. Rendering (a) of the glass sample inside a glass tube as generated from ray-tracing and modeling software Blender. (b) Single projection image as rendered from Blender with the transparent glass sample in front of the random speckle pattern. (c) Resulting displacement map from cross-correlation analysis on the reference image and the projection image shown in (b). (d) 2D contour map of the refractive index integral for the single projection image shown in (b). (e) Final 3D sample after algebraic CT reconstruction utilizing 512 projections.

3.2 Reconstructing object structure

A glass object with a complicated structure (i.e. a hollow body with four leg-like protrusions and half a head) is modeled using Blender. Figure 3(a) shows a rendering of this sample against colored backdrops to help visualize the transparent sample. The glass object is placed in between the reference pattern and the camera, and rotated to capture 512 projections. Figure 3(b) shows a single projection image as rendered from Blender with the glass object placed in front of

the reference pattern. Each projection image is 1920 × 1080 pixels in resolution. For each projection, cross-correlation analysis is conducted using in-house software[24]. This software uses an implementation of sub-pixel interpolation that has been rigorously evaluated[25] to show a practical limit to the error to be approximately 0.05 pixels. The cross-correlation analysis is conducted with an iterative scheme from 128 × 128 pixels to 8 × 8 pixels interrogation regions with a sampling distance of 8 pixels; resulting in a 2D map of 240 × 135 measurements. Figure 3(c) shows the vector map with vectors showing displacement as measured from the cross-correlation analysis. As evident on the vector map, there are some erroneous measurements. This is due to a too large an underlying shift between the reference and projection images for the cross-correlation in the cross-correlation analysis to yield an accurate measurement. The displacement vector field is then analyzed and integrated to determine a 2D map of the refractive index line integrals such as the map shown on figure 3(d). Using 512 projections with 1024 iterations, the glass object is reconstructed using an in-house CT SART routine written using the NVIDIA GPU CUDA architecture. Figure 3(e) shows the 3D reconstructed glass object. The reconstructed glass object closely matches the input object modeled in Blender. However, as evident by the minor reconstruction errors on the tube walls, the erroneous displacement measurements have affected the accuracy of reconstruction. No smoothing routines were implemented at any step in the analysis.

3.3 Determining the resolution of the RIT-CT method

The resolution of the proposed RIT-CT method is tested using a test to determine the modulation transfer function (MTF) by applying RIT-CT to computer-generated images. The MTF is a widely used scientific method of determining the performance of an imaging system. The MTF measures how faithfully the system is able to resolve spatial features in a measurement. Only the resolution of the cross-correlation analysis and refractive index integral estimation processes in the RIT-CT method is tested as the resolution of CT is very well documented. 12 objects with sinusoidal surfaces were modeled using Blender where the frequency of the sine wave ranges from 1 to 23 Hz in increments of 2 Hz. 12 images of 256 × 256 pixels resolution are rendered using Blender for the 12 objects with wavy surfaces of increasing frequencies.

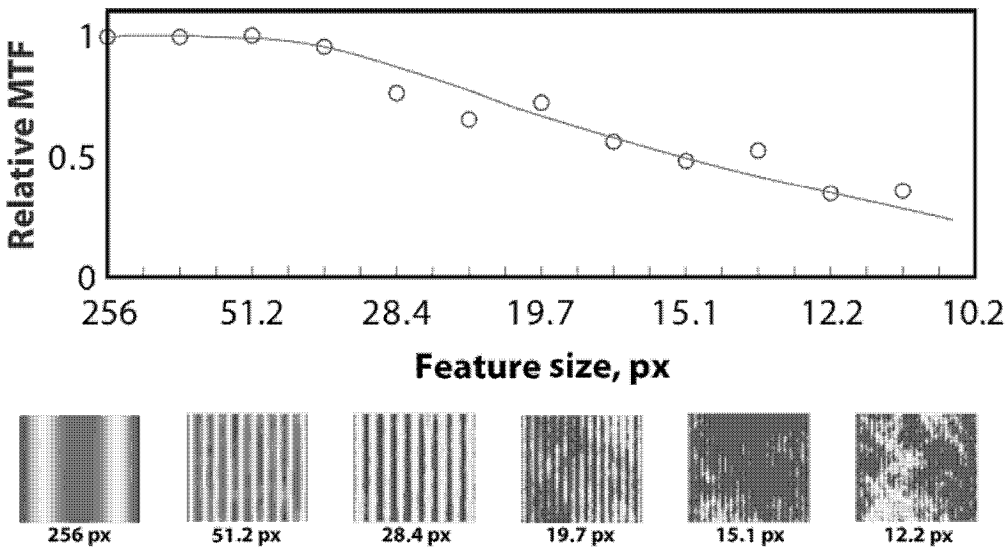

Figure 4. Plot of the relative MTF associated with estimating the refractive index as a function of feature size. This MTF data is obtained for a single 2D projection and does not include the CT step.

For each frequency, the cross-correlation analysis is conducted between the reference and object images with an iterative scheme from 128 × 128 pixels to 8 × 8 pixels interrogation windows with a sampling distance of 2 pixels. Subsequently, the refractive index integral is determined from the resulting displacement map. As the sample thickness is known, the true solution to the sinusoidal refractive index map is readily known for a given frequency. The RMS error between the estimated refractive index integral and the true integral is calculated for each frequency. The MTF is defined as MTF = 1.0 – RMS as the RMS error is representative of the accuracy in estimating the refractive index. 50% modulation is achieved at a spatial frequency of ~17 Hz which has a feature size of ~16 pixels. This is agreeable with the Nyquist sampling theorem as the interrogation window utilized is 8 × 8 pixels and the smallest object resolvable is two times the measurement window.

3.4 Application to synthetic phantom

To test the CT method of RIT-CT in reconstructing the 3D refractive index from 2D projections, the RIT-CT method is applied to a synthetic phantom generated in Blender. This phantom consists two worm-like structures inside a thick hollow sphere. For complexity for the reconstruction, the hollow sphere has a portion cut out exposing the interior structures to the outside. All the components of the phantom are completely transparent. Figure 5(a) shows a rendering of the phantom colored by the refractive index. The smaller of the interior components of the phantom has a refractive index of 0.99 while the other component inside the phantom and the hollow sphere have a refractive index of 1.01. 128 projection images of the phantom, each 1024 × 1024 pixels in resolution, are generated using Blender. Cross-correlation analysis is conducted with an iterative scheme from 128 × 128 pixels down to 8 × 8 pixels interrogation windows with a sampling distance of 8 pixels, resulting in a 2D map with 128 × 128 measurements.

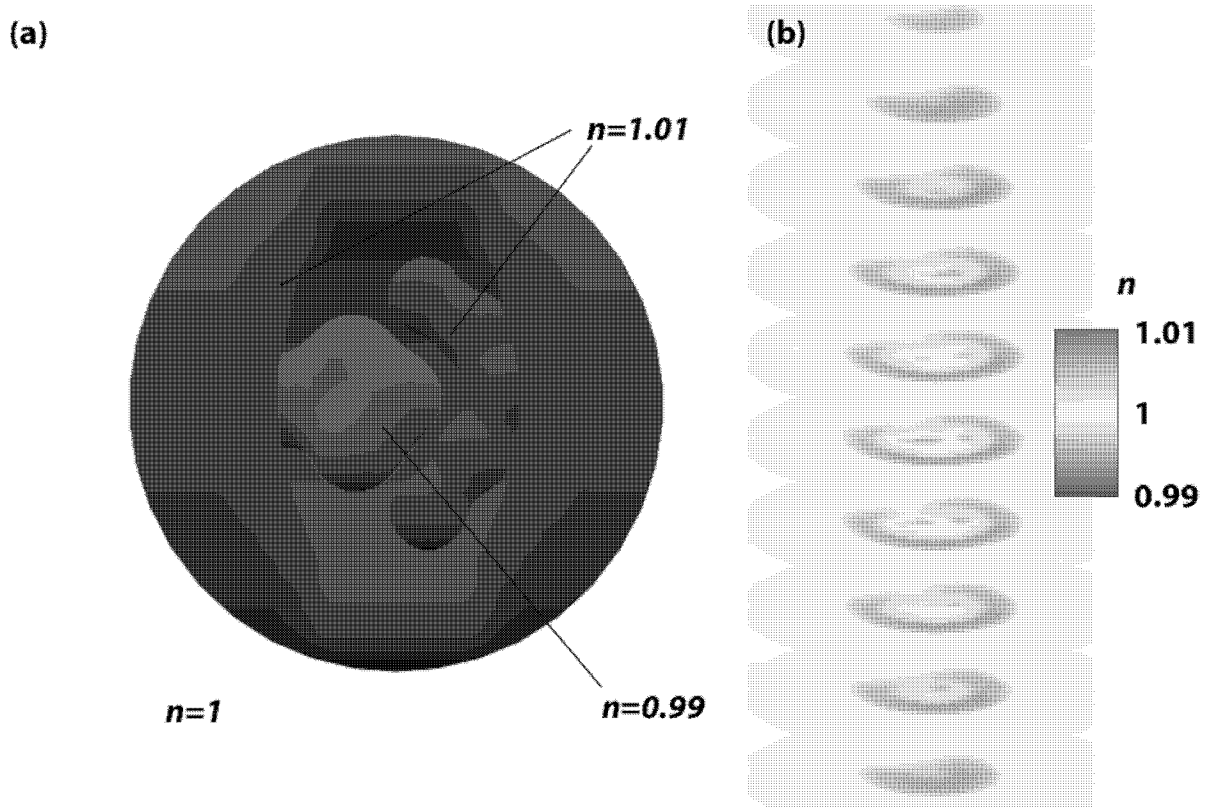

Figure 5. Synthetic phantom created using Blender to test the refractive index measurement of RIT-CT. This phantom consists of two worm-like structures that have different refractive indices, encased in a hollow thick walled sphere. The hollow sphere has a portion sliced out to provide an interesting test for RIT-CT. (a) Rendering of the phantom with colored contours showing the refractive index of its specific parts. (b) Slices showing the 3D reconstructed refractive index field from RIT. For clarity, only every 5 slices in the vertical direction is shown.

The refractive index integrals are determined for these 128 × 128 points for each projection angle and the 3D refractive index map is reconstructed utilizing all 128 projections with a SART routine. Figure 5(b) shows the volumetric slices of the reconstructed 3D refractive index field with color contours depicting the refractive index. Only every 5 projections in the stacking direction are shown for the purpose of clarity. As evident by the reconstruction, there are reconstruction artifacts present in the final reconstruction. This could be reduced using smoothing filters, larger number of projections and larger number of iterations. However, the refractive indices of the components in the phantom are closely matched.

4. CONCLUSION

A novel diffraction-based method capable of 3D refractive index measurements is presented. This method, called Reference Image Topography - Computed Tomography (RIT-CT) uses Particle Image Velocimetry, a modified variation of Reference Image Topography[10], [11] and CT for imaging samples that are transparent to the imaging spectrum to obtain 3D quantitative information. A series of tests utilizing *in silico* models is used to test the RIT-CT method. This method uses a simple setup and is capable of efficient utilization of light due to the absence of diffraction gratings, attenuation grids or analyzer crystals in the optical configuration. Hence, the RIT-CT method can be applied for the volumetric imaging of dynamic biological samples.

ACKNOWLEDGEMENTS

The authors would like to acknowledge the insightful discussions with Stephen Dubsky. Support from the Australian Research Council, the National Health and Medical Research Council, the NCI National Computational Merit Allocation Scheme and the VLSCI Resource Allocation Scheme is gratefully acknowledged.

REFERENCES

[1] S. Dubsky, S. B. Hooper, K. K. W. Siu, and A. Fouras, "Synchrotron-based dynamic computed tomography of tissue motion for regional lung function measurement," *J. R. Soc. Interface*, Apr. 2012.

[2] A. Wanninger, "The application of confocal microscopy and 3D imaging software in Functional, Evolutionary, and Developmental Zoology: reconstructing myo- and neurogenesis in space and time," *Modern Research and Educational Topics in Microscopy. Formatex*, pp. 353–361, 2007.

[3] J. Sharpe, U. Ahlgren, P. Perry, B. Hill, A. Ross, J. Hecksher-Sørensen, R. Baldock, and D. Davidson, "Optical Projection Tomography as a Tool for 3D Microscopy and Gene Expression Studies," *Science*, vol. 296, no. 5567, pp. 541–545, Apr. 2002.

[4] A. Momose, T. Takeda, Y. Itai, and K. Hirano, "Phase–contrast X–ray computed tomography for observing biological soft tissues," *Nature Medicine*, vol. 2, no. 4, pp. 473–475, Apr. 1996.

[5] A. Fouras, B. Allison, M. Kitchen, S. Dubsky, J. Nguyen, K. Hourigan, K. Siu, R. Lewis, M. Wallace, and S. Hooper, "Altered Lung Motion is a Sensitive Indicator of Regional Lung Disease," *Annals of Biomedical Engineering*, vol. 40, no. 5, pp. 1160–1169, 2012.

[6] S. W. Wilkins, T. E. Gureyev, D. Gao, A. Pogany, and A. W. Stevenson, "Phase-contrast imaging using polychromatic hard X-rays," *Nature*, vol. 384, pp. 335–338, 1996.

[7] E. Cuche, F. Bevilacqua, and C. Depeursinge, "Digital holography for quantitative phase-contrast imaging," *Opt. Lett.*, vol. 24, no. 5, pp. 291–293, Mar. 1999.

[8] T. Nakamura and C. Chang, "Quantitative x-ray differential-interference-contrast microscopy with independently adjustable bias and shear," *Phys. Rev. A*, vol. 83, no. 4, p. 043808, Apr. 2011.

[9] B. Atcheson, I. Ihrke, W. Heidrich, A. Tevs, D. Bradley, M. Magnor, and H.-P. Seidel, "Time-resolved 3D Capture of Non-stationary Gas Flows," *ACM Transactions on Graphics (Proc. SIGGRAPH Asia)*, vol. 27, no. 5, p. 132, 2008.

[10] A. Fouras, D. Lo Jacono, G. J. Sheard, and K. Hourigan, "Measurement of instantaneous velocity and surface topography in the wake of a cylinder at low Reynolds number," *Journal of Fluids and Structures*, vol. 24, no. 8, pp. 1271–1277, 2008.

[11] A. Fouras, K. Hourigan, M. Kawahashi, and H. Hirahara, "An Improved, Free Surface, Topographic Technique," *Journal of Visualization*, vol. 9, no. 1, pp. 49–56, Jan. 2006.

[12] K. S. Morgan, D. M. Paganin, and K. K. W. Siu, "Quantitative single-exposure x-ray phase contrast imaging using a single attenuation grid," *Optics Express*, vol. 19, no. 20, p. 19781, Sep. 2011.

[13] S. Bérujon, E. Ziegler, R. Cerbino, and L. Peverini, "Two-Dimensional X-Ray Beam Phase Sensing," *Phys. Rev. Lett.*, vol. 108, no. 15, p. 158102, Apr. 2012.

[14] J. H. Massig, "Measurement of Phase Objects by Simple Means," *Appl. Opt.*, vol. 38, no. 19, pp. 4103–4105, Jul. 1999.

[15] C. D. Perciante and J. A. Ferrari, "Visualization of Two-Dimensional Phase Gradients by Subtraction of a Reference Periodic Pattern," *Appl. Opt.*, vol. 39, no. 13, pp. 2081–2083, May 2000.

[16] I. Ng, V. Kumar, G. Sheard, K. Hourigan, and A. Fouras, "Experimental study of simultaneous measurement of velocity and surface topography: in the wake of a circular cylinder at low Reynolds number," *Experiments in Fluids*, vol. 50, no. 3, pp. 587–595, 2011.
[17] V. Kumar, I. Ng, G. J. Sheard, E. Brocher, K. Hourigan, and A. Fouras, "Application of Particle Image Velocimetry and Reference Image Topography to jet shock cells using the hydraulic analogy," *Exp. Fluids*, vol. 51, no. 2, pp. 543–551, Aug. 2011.
[18] T. Ackerly, J. C. Crosbie, A. Fouras, G. J. Sheard, S. Higgins, and R. A. Lewis, "High resolution optical calorimetry for synchrotron microbeam radiation therapy," *Journal of Instrumentation*, vol. 6, no. 03, pp. P03003–P03003, Mar. 2011.
[19] K. S. Morgan, D. M. Paganin, and K. K. W. Siu, "X-ray phase imaging with a paper analyzer," *Applied Physics Letters*, vol. 100, no. 12, pp. 124102–124102–4, Mar. 2012.
[20] S. Dubsky, R. A. Jamison, S. C. Irvine, K. K. W. Siu, K. Hourigan, and A. Fouras, "Computed tomographic x-ray velocimetry," *Applied Physics Letters*, vol. 96, no. 2, p. 023702, 2010.
[21] W. Choi, C. Fang-Yen, K. Badizadegan, S. Oh, N. Lue, R. R. Dasari, and M. S. Feld, "Tomographic phase microscopy," *Nature Methods*, vol. 4, no. 9, pp. 717–719, Sep. 2007.
[22] A. Maksimenko, M. Ando, S. Hiroshi, and T. Yuasa, "Computed tomographic reconstruction based on x-ray refraction contrast," *Applied Physics Letters*, vol. 86, no. 12, p. 124105, 2005.
[23] C. R. Samarage, J. Carberry, K. Hourigan, and A. Fouras, "Optimisation of temporal averaging processes in PIV," *Experiments in Fluids*, vol. 52, no. 3, pp. 617–631, 2012.
[24] A. Fouras, D. Lo Jacono, and K. Hourigan, "Target-free Stereo PIV: a novel technique with inherent error estimation and improved accuracy," *Experiments in Fluids*, vol. 44, pp. 317–329, 2007.
[25] A. Fouras, J. Dusting, and K. Hourigan, "A simple calibration technique for stereoscopic particle image velocimetry," *Experiments in Fluids*, vol. 42, no. 5, pp. 799–810, 2007.